Talanta 84 (2011) 1384–1389

Contents lists available at ScienceDirect

Talanta

journal homepage: www.elsevier.com/locate/talanta

Electrochemical detection on electrowetting-on-dielectric digital microfluidic chip

Chanpen Karuwan[a], Kreeta Sukthang[b], Anurat Wisitsoraat[a], Ditsayut Phokharatkul[a], Viyapol Patthanasettakul[a], Wishsanuruk Wechsatol[b], Adisorn Tuantranont[a,*]

[a] Nanoelectronics and MEMS Laboratory, National Electronics and Computer Technology Center, Pathumthani 12120, Thailand
[b] Department of Mechanical Engineering, King Mongkut's University of Technology, Thonburi 126 Prachauthit Road, Bangmod Thung Kharu District, Bangkok 10140, Thailand

ARTICLE INFO

Article history:
Available online 28 April 2011

Keywords:
Electrowetting-on-dielectric
Digital microfluidic
Electrochemical detection

ABSTRACT

In this work, the use of three-electrode electrochemical sensing system with an electrowetting-on-dielectric (EWOD) digital microfluidic device is reported for quantitative analysis of iodide. T-junction EWOD mixer device was designed using arrays of 50-μm spaced square electrodes for mixing buffer reagent and analyte droplets. For fabrication of EWOD chips, 5-μm thick silver EWOD electrodes were formed on a glass substrate by means of sputtering and lift-off process. PDMS and Teflon thin films were then coated on the electrodes by spin coating to yield hydrophobic surface. An external three-electrode system consisting of Au working, Ag reference and Pt auxiliary wires were installed over EWOD electrodes at the end of T-junction mixer. In experiment, a few-microliter droplets of Tris buffer and iodide solutions were moved toward the mixing junction and transported toward electrochemical electrodes by EWOD process. A short processing time within seconds was achieved at EWOD applied voltage of 300 V. The analyte droplets mixed with different concentrations were successfully analyzed by cyclic voltametry. Therefore, the combination of EWOD digital microfluidic and electrochemical sensing system has successfully been demonstrated for rapid chemical analysis with minimal reagent consumption.

1. Introduction

In recent years, there has been a great interest in miniaturized analysis systems for chemical and biological applications [1]. These systems and devices, also well known as lab-on-a-chip (LOC), offer several advantages including low sample/reagent consumption, fast analysis, high throughput and automation capability. Conventional microfluidic platforms are based on continuous flow scheme operated by fluid pressure [2] or electrokinetic actuation [3]. Recently, a new category of microfluidics, called droplet-based microfluidics, has been developed. In contrary to conventional continuous flow scheme, droplets of samples/reagent are formed instead of continuous stream, which results in lower sample/reagent consumption. There are two main types, namely continuous and discrete droplet based microfluidics. In the continuous type, droplets are generated and transported along microfluidic channels by flowing sample/reagent into an immiscible carrier fluid that separates and encapsulates continuous solution stream into microdroplets. The main benefit of this method is very high throughput. In the discrete approach, samples/reagent are formed, manipulated and analyzed as isolated microdroplets with no need of carrier and microchannel. This method has several advantages over continuous-type systems, including extremely low sample/reagent consumption, parallel processing ability, reconfigurability, architectural scalability and ease of fabrication [4]. Thus, droplet-based microfluidic systems have increasingly gained interest in various applications. Due to the architectural similarities with digital microelectronic systems, it is often referred as "digital microfluidics".

A variety of droplet manipulation technologies have been demonstrated including surface acoustic wave [5–8], thermocapillary forces [9,10], electrowetting-on-dielectric (EWOD) [11–15], dielectrophoresis (DEP) [16–21] and magnetic forces [22,23]. Among them, EWOD is one of the most promising techniques because of fast response time, easy implementation, low power consumption, no joule heating effect and large force at the millimeter to micrometer scales. The principle of electrowetting is the modulation of interfacial tension between a conducting liquid phase and an insulated solid electrode by the application of a high electric potential between the two. EWOD has been employed for a variety of droplet manipulations such as transporting, merging, mixing and splitting [4,24–26]. However, there has been relatively few reports on coupling of EWOD devices with detection components. Among a variety of detection methods, electrochemical technique is highly promising for microsystem applications because of its high performance detection, simplicity and scala-

* Corresponding author. Tel.: +66 2 564 6900; fax: +66 2 564 6756.
E-mail address: adisorn.tuantranont@nectec.or.th (A. Tuantranont).

0039-9140/$ – see front matter © 2011 Elsevier B.V. All rights reserved.
doi:10.1016/j.talanta.2011.03.073

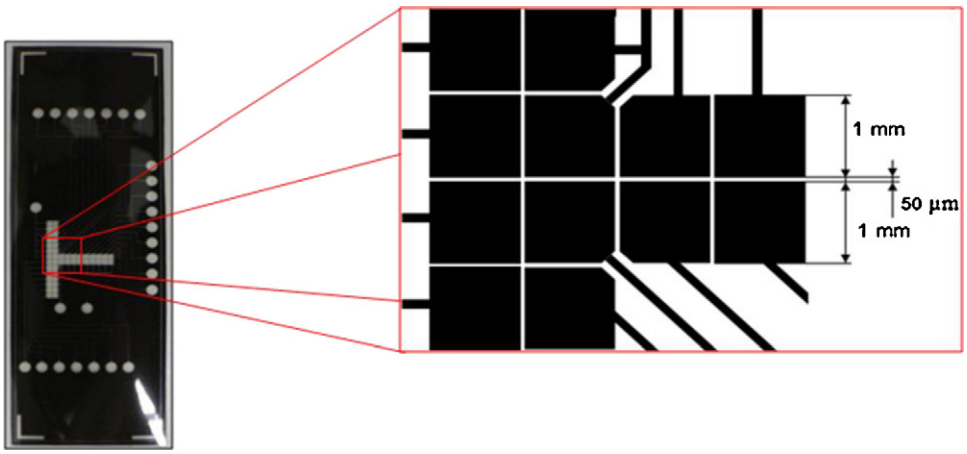

Fig. 1. The layout of electrodes for T-junction EWOD mixer device.

bility. Nevertheless, there has been very few reports on coupling of electrochemical detection scheme with EWOD microfluidic device [27,28].

In this work, the coupling of three-electrode electrochemical sensing system with EWOD digital microfluidic devices is developed for quantitative analysis of an analyte. T-junction EWOD mixer device is combined with external three-electrode system for detection of iodide microdroplets using cyclic voltametry. The characteristics of EWOD device and electrochemical detection of iodide microdroplets are studied.

2. Experimental

2.1. EWOD chip design and fabrication

T-junction EWOD mixer device is designed on a glass substrate for buffer reagent and analyte droplets mixing. The layout of electrodes for T-junction EWOD mixer device is shown in Fig. 1. EWOD electrodes are designed as closely spaced electrode arrays. To obtain effective EWOD actuation, the ratio of the gap between square electrodes (g) and the width of square electrode (w) should be minimal because the contact angle of the wetting droplet decreases with g/w ratio and it is easier for the droplet to move when the contact angle reduces [29]. However, g/w ratio is set to be 5% in order to avoid dielectric breakdown of the underlying glass substrate. Due to photolithographic constraints, the gap between square electrodes and the width of square electrode are designed to be 50 μm and 1 mm, respectively. Silver is selected as electrode material due to its high electrical conductivity.

The EWOD silver electrode was fabricated on glass substrate by lift-off process. The surface of glass substrate was cleaned with acetone and methanol. The AZ-P4620 photoresist was then deposited by spin coating at 1250 rpm for 30 s and then soft-baked at 90 °C for 3 min. Next, the photoresist was exposed to UV light under the designed photomask using MJB4 mask aligner (SUSS Microtec, Germany). It was then developed and cleaned with deionized water. The glass substrate with photoresist pattern is shown in Fig. 2(a). The photoresist was hard-baked at 120 °C for 3 min to make it hard enough for subsequent sputtering deposition. Next,

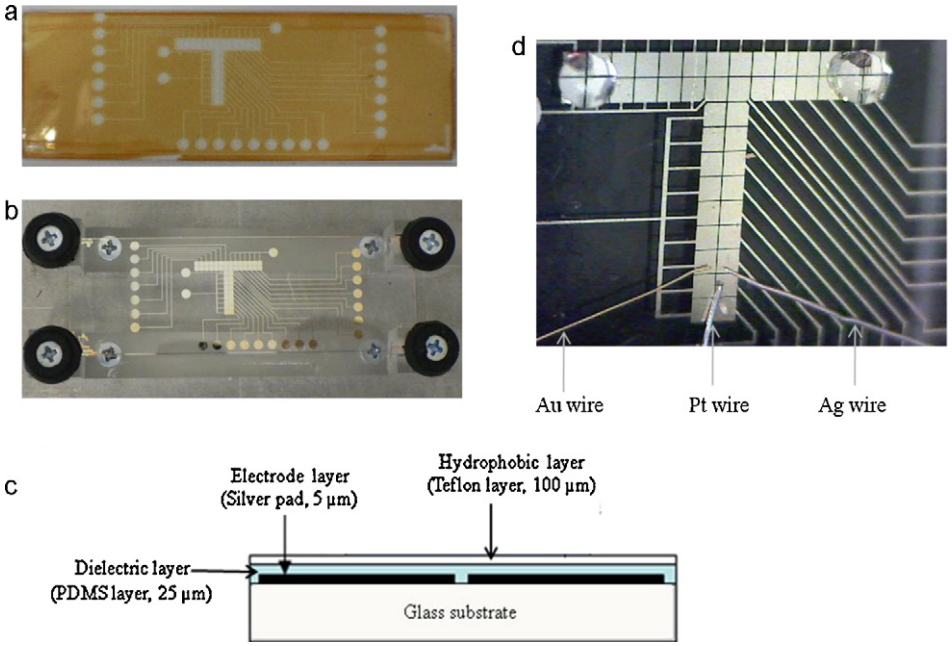

Fig. 2. (a) Photograph of glass substrate with photoresist pattern, (b) photograph of glass chip with EWOD silver electrodes, (c) cross-sectional structure of EWOD chip and (d) photograph of EWOD chip with three electrode system containing gold (Au) working electrode, platinum (Pt) auxiliary electrode and silver (Ag) reference electrode at the end of T-junction.

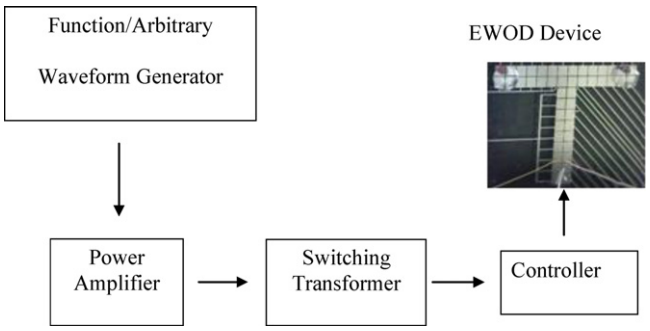

Fig. 3. Schematic diagram of the control system for EWOD device.

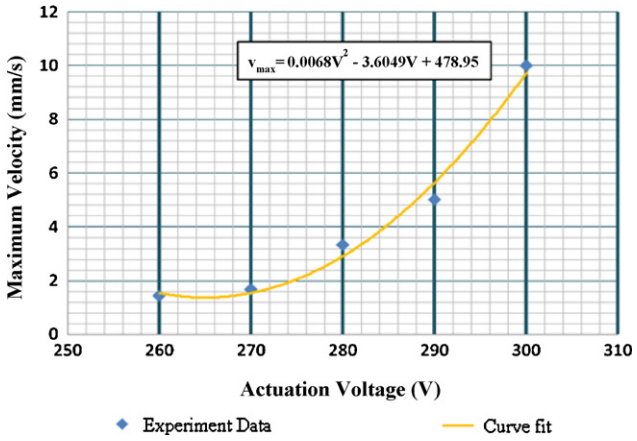

Fig. 4. Maximum velocity of droplet vs. actuation voltage of EWOD device.

0.1-μm thick chromium and 5-μm thick silver films were successively sputtered by DC sputtering process at an argon pressure of 10^{-2} mbar. Next, the metal film on photoresist was lifted off by ultrasonication in acetone for 15 min.

Polydimethylsiloxane (PDMS) dielectric layer (Fig. 2(c)) was then coated on the EWOD electrode by spin coating. PDMS was prepared by mixing of silicon elastomer base and silicon elastomer curing agent with a volumetric ratio of 10:1. The PDMS was spin-coated at 4000 rpm for 30 s on top of the glass surface to form a 5 μm thick dielectric layer. The glass chip was baked at 95 °C for 60 min on a hot plate to cure PDMS. Finally, Teflon AF hydrophobic layer was spin-coated at 1000 rpm for 30 s to generate a 100 nm thick hydrophobic layer. Teflon AF solution grade 400S1-100-1 was used because of its superior hydrophobic and dielectric properties compared to normal Teflon [30]. The glass chip was baked again at 95 °C for 60 min to cure Teflon AF. The purpose of hydrophobic layer is to provide suitable contact angle and mobility for a droplet.

2.2. Electrochemical system

An external three-electrode electrochemical sensing system consisting of Au working, Ag reference and Pt auxillary wires was installed over EWOD electrodes at the end of T-junction mixer as shown in Fig. 2d. A potentiostat, μ-autolab Type III (Metrohm, Switzerland) was used for all the cyclic voltammetric (CV) studies.

2.3. Chemicals

All of chemicals used in this work were analytical grade. Standard solutions of iodide were purchased from Sigma (USA). Various buffers including acetate (pH 5) and phosphate (pH 6–8) were purchased from Merck (Germany). Tris buffer solution (pH 9) was prepared from tris (hexahydroxy) aminomethane and 1.0 M hydrochloric acid (HCl) (Lab Scan, Ireland). The stock solution (0.01 mol l^{-1}) of iodide was prepared by dissolving required amount of iodide in deionized–distilled water. Glass substrates, Photoresist (AZ®P4620), Telfon AF and PDMS were purchased from Superior (Germany), AZ electronic materials (USA), Dupont (USA) and Dow Chemical (USA), respectively.

2.4. Experimental procedure

EWOD device was driven by a control system as shown in Fig. 3. A small signal from function/arbitrary waveform generator was amplified by a power amplifier, which drove a switching transformer. The switching transformer was used to supply a high voltage of 300 V. The high voltage was applied via a high-speed controller, which provided proper switching to EWOD electrodes according to command set by users. A droplet could be forced to move forward and to turn left or right by changing the direction and position of applied voltage along the line of electrodes. In addition, the droplet movement could be accelerated or decelerated by changing the controlled time of applied voltage on each electrode. In this experiment, the signal frequency was set at 400 Hz, which was selected for suitable mobility of droplets.

For iodide analysis, a droplet of KI solution and a droplet of Tris buffer solution were dropped from auto pipette tips on two ends of T arms as shown in Fig. 3. Both droplets were then moved to the mixing junction by EWOD control voltages. After droplets were mixed, the combined droplet was transported to the three-electrode system at the end of T junction and CV measurement was performed using potential window between 0 and 1.2 V. The process was repeated with different droplet sizes to vary iodide concentration of the final droplet. The concentration was determined from the product of initial iodide concentration and the ratio of analyte's droplet volume and the final volume of the mixed droplet.

3. Results and discussions

3.1. Effect of applied voltage on the velocity of droplet

To determine suitable actuation voltage for the EWOD device, maximum droplet velocity was measured as a function of applied voltage. To find maximum droplet velocity, the controlled time of applied voltage on each electrode was increased from zero until the droplet moved from one electrode to adjacent electrode. The maximum velocity was then estimated from the distance that droplet moved (equal to the gap plus the width of electrode) and the minimum time required to move the droplet at each applied voltage. The maximum velocity of droplet as a function of actuation voltage of EWOD device is shown in Fig. 4. It can be seen that the maximum velocity increases rapidly when the applied voltage is more than 270 V. An empirical relationship of the maximum velocity and applied voltage is found to be quadratic order by regression curve fitting and is given by:

$$v_{max} = 0.0068V^2 - 3.6049V + 478.95$$

where v_{max} is the maximum velocity of water droplet (mm/s) and V is the actuation potential (V). The maximum velocity is a second order function of EWOD potential because EWOD force acting upon the droplet is proportional to the square of applied voltage [13,14] and maximum velocity varies linearly with force at a given time.

3.2. EWOD processing

Droplets of iodide and Tris buffer solutions were successfully manipulated, mixed and transported for electrochemical detection

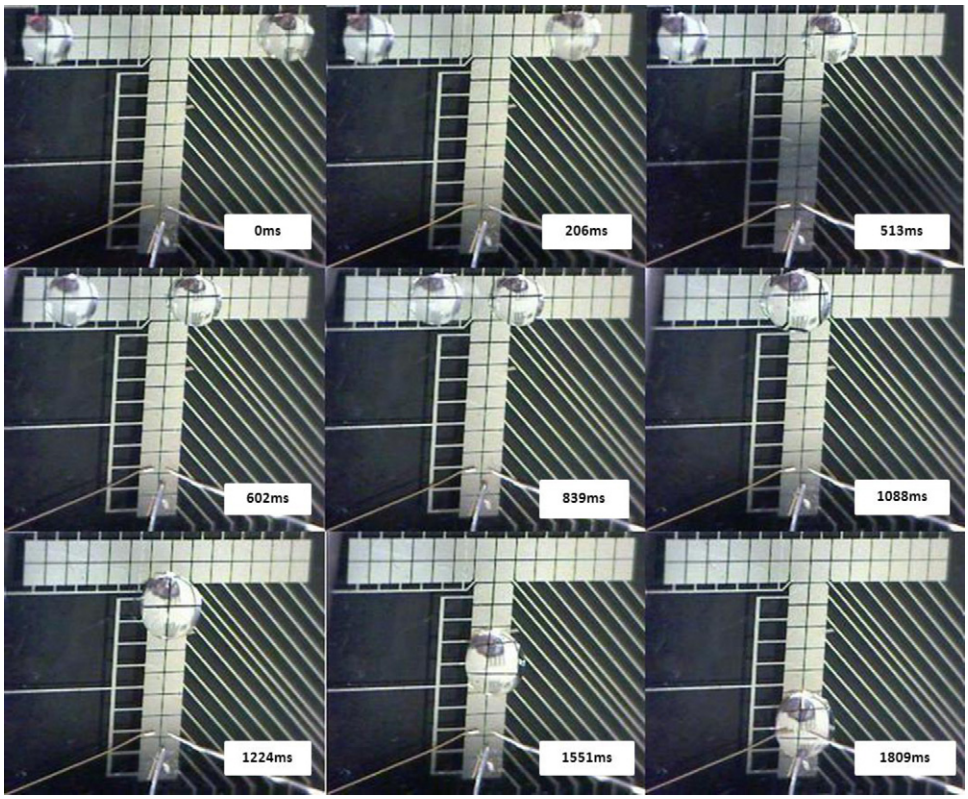

Fig. 5. Snapshots of sample and reagent droplets at various steps on EWOD device.

by EWOD process. Fig. 5 shows the snapshots of sample and reagent droplets at various steps on EWOD device. The concentration of the iodide droplet is 1 mM and the applied voltage is 300 V. It can be seen that the transport time before merging and detection are ~0.8 s and ~1.8 s, respectively. The processing time within seconds is considered short and high throughput can be achieved by EWOD. Nevertheless, it can be inferred from Fig. 4 that processing time may be further reduced to an order of milliseconds, which will be comparable to continuous flow system, by increasing applied voltage that will result in quadratic increase of maximum velocity.

3.3. Electrochemical detection of iodide droplets

3.3.1. pH dependence study

The effect of pH on response to 1 mM iodide droplet was evaluated in order to select an optimum pH value. Fig. 6 shows the cyclic voltammograms of 1 mM iodide droplets in buffers with different pHs. The Au electrodes exhibit well-defined CV of iodide with two oxidation peaks for all pHs except pH 8 that exhibit only one broad oxidation peak. pH 6 is selected for further studies on Au electrode due the observed sharp peak at 0.75 V.

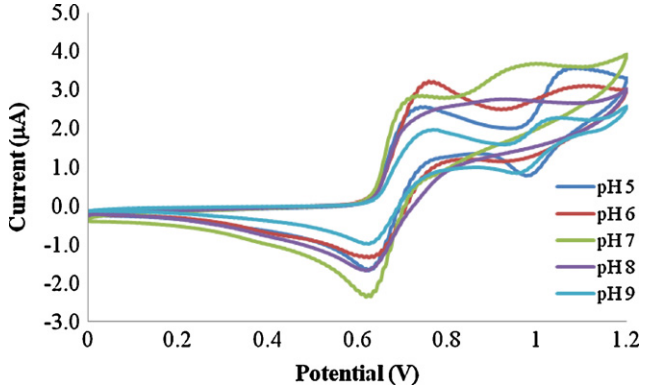

Fig. 6. The cyclic voltammograms that were obtained from EWOD chip for 1 mM iodide in various buffers (pH 5–9). The scan rate was fixed at 0.1 V/s.

3.3.2. Scan rate dependence study

Cyclic voltammograms of 1 mM iodide droplets of Au electrode were investigated at different scan rates and the results are displayed in Fig. 7(a). Fig. 7(b) shows the relationship between the second oxidation peak current and the square root of the scan rate. It is evident that peak current at the second oxidation peak varies linearly with the square root of scan rate. The slope of regression line is 6.47 μA $(s/V)^{1/2}$ and correlation coefficient (r^2) is 0.998. This confirms that the current is limited by seminfinite linear diffusion of iodide on the Au electrode [31].

3.3.3. Analytical features

The analytical performances of the EWOD electrochemical system for iodide droplet detection were characterized by CV at different concentrations ranging from 10 to 100 μM. Linear concentration dependence or dynamic range was observed between 10 and 100 μM. The regression equation was given by $y = 0.0007x + 0.0058$ ($r^2 = 0.9917$), where y and x were the height of peak current (μA) and iodide concentration (μM), respectively. The slope of the equation was corresponding to a linear sensitivity of 0.0007 μA/μM. The detection limit (3S/N) was 2.76 μM. The noise value (N) was measured by taken peak–peak amplitude of sinusoidal noise in the base line region of CV curve. The stability was checked by recording successive CVs. The electrode remained stable after 20 successive cycles with relative standard deviation (RSD) of 3.3% ($n = 20$). The total analysis time including droplet mixing and CV measurement was approximately 12 s. Therefore, the analytical

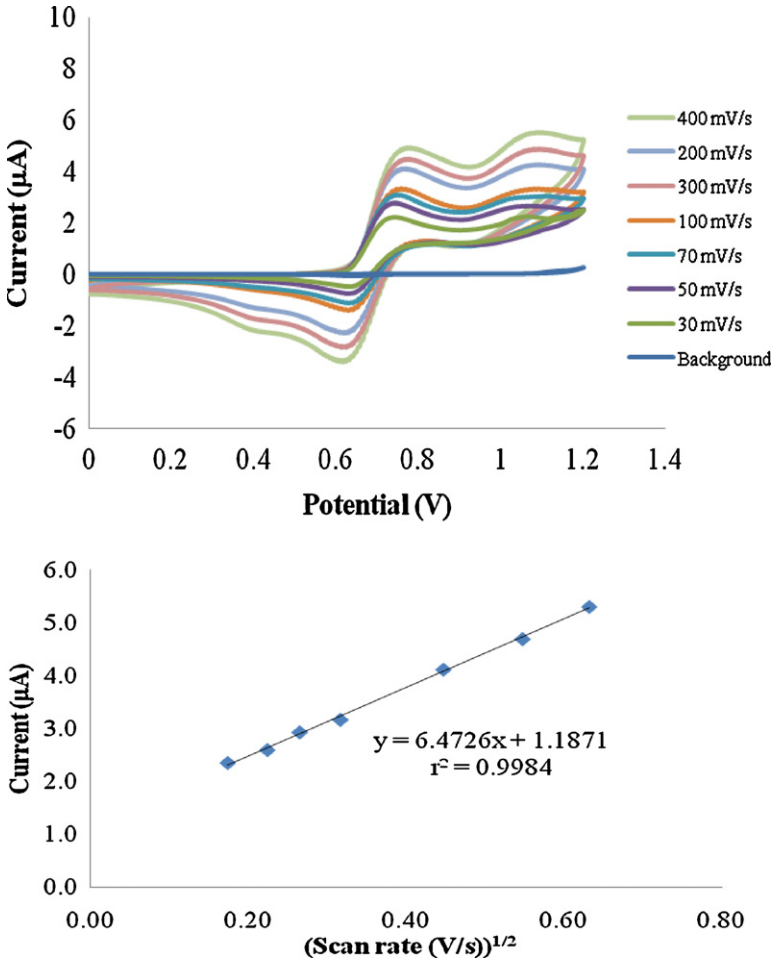

Fig. 7. (a) Cyclic voltammograms, obtained at various potential scan rates for 1 mM iodide in 1 mM phosphate buffer (pH 6) of Au electrode. (b) The relationship between the second oxidation peak current and the square root of the scan rate.

performances are attractive for high throughput real world analysis of iodide in pharmaceutical and medical applications.

4. Conclusions

In conclusion, the coupling of three-electrode electrochemical sensing system with a droplet-based EWOD microfluidic device is demonstrated for quantitative analysis of iodide. An external three-electrode electrochemical sensing system consisting of Au working, Ag reference and Pt auxiliary wires was suspended at the end of T-junction EWOD mixing device. Microdroplet of Tris buffer and potassium iodide solution were mixed and successfully detected by cyclic voltametry with short processing time within seconds. The combination of EWOD digital microfluidic and electrochemical sensing system is illustrated as a promising method for rapid chemical analysis with minimal reagent consumption.

Acknowledgements

Adisorn Tuantranont would like to express his gratitude for Researcher Career Development Grant from Thailand Research Fund (TRF). Wishsanuruk Wechsatol would also like to acknowledge the financial support from Industry/University Cooperative/Research Center in HDD Advanced Manufacturing and National Electronics and Computer Technology Center, National Science and Technology Development Agency.

References

[1] E. Verpoorte, Electrophoresis 23 (2002) 677–712.
[2] C. Karuwan, A. Wisitsoraat, T. Maturos, D. Phokharatkul, A. Sappat, K. Jaruwongrungsee, T. Lomas, A. Tuantranont, Talanta 79 (2009) 995–1000.
[3] J. Wang, Electrophoresis 23 (2002) 713–718.
[4] M.G. Pollack, A.D. Shendorov, R.B. Fair, Lab Chip 2 (2002) 96–101.
[5] D. Beyssen, L.L. Brizoual, O. Elmazria, P. Alnot, Sens. Actuators B 118 (2006) 380–385.
[6] Z. Guttenberg, H. Müller, H. Habermüller, A. Geisbauer, J. Pipper, J. Felbel, M. Kielpinski, J. Scriba, A. Wixforth, Lab Chip 5 (2005) 308–317.
[7] J. Shi, D. Ahmed, X. Mao, S.-C.S. Lin, A. Lawit, T.J. Huang, Lab Chip 9 (2009) 2890–2895.
[8] T. Franke, A.R. Abate, D.A. Weitz, A. Wixforth, Lab Chip 9 (2009) 2625–2627.
[9] J.Z. Chen, S.M. Troian, A.A. Darhuber, S. Wagner, J. Appl. Phys. 97 (2005) 014906.
[10] A.T. Ohta, A. Jamshidi, J.K. Valley, H.-Y. Hsu, M.C. Wu, Appl. Phys. Lett. 91 (2007) 07413.
[11] D. Brassardab, L. Malicac, F. Normandina, M. Tabrizianc, T. Veres, Lab Chip 8 (2008) 1342–1349.
[12] S.K. Cho, H. Moon, C.-J. Kim, J. MEMS 12 (2003) 70–80.
[13] M. Vallet, B. Berge, L. Vovelle, Polymer 37 (1996) 2465–2470.
[14] M. Abdelgawad, S.L.S. Freire, H. Yang, A.R. Wheeler, Lab Chip 8 (2008) 672–677.
[15] J. Gong, C.-J. Kim, Lab Chip 8 (2008) 898–906.
[16] S.-Y. Park, C. Pan, T.-H. Wu, C. Kloss, S. Kalim, C.E. Callahan, M. Teitell, E.P.Y. Chiou, Appl. Phys. Lett. 92 (2008) 151101.
[17] J.A. Schwartz, J.V. Vykoukal, P.R.C. Gascoyne, Lab Chip 4 (2004) 11–17.
[18] S.-Y. Park, S. Kalim, C. Callahan, M.A. Teitell, E.P.Y. Chiou, Lab Chip 9 (2009) 3228–3235.
[19] K. Ahn, C. Kerbage, T.P. Hunt, R.M. Westervelt, D.R. Link, D.A. Weitz, Appl. Phys. Lett. 88 (2006) 024104.
[20] O.D. Velev, B.G. Prevo, K.H. Bhatt, Nature 426 (2003) 515–516.
[21] J.-C. Baret, O.J. Miller, V. Taly, M. Ryckelynck, A. El-Harrak, L. Frenz, C. Rick, M.L. Samuels, J.B. Hutchison, J.J. Agresti, D.R. Link, D.A. Weitz, A.D. Griffiths, Lab Chip 9 (2009) 1850–1858.
[22] Z.-G. Guo, F. Zhou, J.-C. Hao, Y.-M. Liang, W.T.S. Huck, W.-M. Liu, Appl. Phys. Lett. 89 (2006) 081911.

[23] M. Okochi, H. Tsuchiya, F. Kumazawa, M. Shikida, H. Honda, J. Biosci. Bioeng. 109 (2010) 193–197.
[24] S.-K. Cho, H. Moon, C.-J. Kim, Microelectromech. Syst. 12 (2003) 32–52.
[25] P.Y. Paik, V.K. Pamula, M.G. Pollack, R.B. Fair, Lab Chip (2003) 28–33.
[26] P.Y. Paik, V.K. Pamula, R.B. Fair, Lab Chip 3 (2003) 253–259.
[27] P. Dubois, G. Marchand, Y. Fouillet, J. Berthier, T. Douki, F. Hassine, S. Gmouh, M. Vaultier, Anal. Chem. 78 (2006) 4909–4917.
[28] J.L. Poulos, W.C. Nelson, T.J. Jeon, C.C. Kim, J.J. Schmidt, Appl. Phys. Lett. 95 (2009), 13706-13703.
[29] U.C. Yi, C.J. Kim, J. Micromech. Microeng. 16 (2006) 2053–2059.
[30] P. Resnick, W. Buck, in: Hougham et al., Fluoropolymers 2: Properties, Plenum Press, New York, 1999, pp. 25–33.
[31] S. Gottesfeld1, S.W. Feldberg, J. Electroanal. Chem. Interface Electrochem. 194 (1) (1985) 1–10.